Zekeriya Parlak[1]
e-mail: zparlak@sakarya.edu.tr

Tahsin Engin
e-mail: engint@sakarya.edu.tr

Department of Mechanical Engineering,
Sakarya University,
Sakarya 54187, Turkey

İsmail Şahin
Vocational School of Akyazi,
Sakarya University,
Sakarya 54405, Turkey
e-mail: isahin@sakarya.edu.tr

Optimal Magnetorheological Damper Configuration Using the Taguchi Experimental Design Method

Magnetorheological (MR) dampers have attracted the interest of suspension designers and researchers because of their variable damping feature, mechanical simplicity, robustness, low power consumption and fast response. This study deals with the optimal configuration of an MR damper using the Taguchi experimental design approach. The optimal solutions of the MR damper are evaluated for the maximum dynamic range and the maximum damper force separately. The MR dampers are constrained in a cylindrical container defined by radius and height. The optimal damper configurations obtained from this study are fabricated and tested for verification. The verification tests show that the dampers provide the specified damper force and dynamic range.
[DOI: 10.1115/1.4024719]

1 Introduction

Semi-active controllable devices with magnetorheological (MR) fluid have received significant attention, especially for transportation vehicles, building suspensions, and biomedical applications, in the last two decades because of their unique advantages. MR fluids are suspensions of magnetically polarizable particles, a few microns in size, dispersed in a carrying liquid, such as mineral oil or silicon oil. When a magnetic field is applied to the fluid, particles in the fluid form chains and the suspension become a semisolid material in a few milliseconds. Exposed to the magnetic field, an MR fluid behaves as a non-Newtonian fluid with controllable viscosity. However, if the magnetic field is removed, the suspension returns to a Newtonian fluid. The transition between these two phases is highly reversible, which provides a unique feature, magnetic-field controllability of the flow, in MR fluids.

Recently, some studies have focused on the geometric optimization of MR devices. Many factors must be considered when developing optimal designs of MR dampers, making the problem challenging when using conventional optimization methods. The framework of the optimization procedure should be based on physical design requirements. The fail-safe design feature is accomplished by selecting the appropriate channel flow geometry to obtain the minimum required viscous (passive) damping force for the zero magnetic field condition [1].

Controllability of MR devices is provided by applying different magnetic fields across a gap through which the MR fluid flows. In numerous papers, single rectangular [2–4] and annular ducts [5–9] were employed in the devices. Similarly, Stanway et al. [10] and Namuduri et al. [11] proposed multiple concentric annular gaps. To provide a magnetic field, a coil and a magnetic flux guide is needed, which can have implications for the weight, size and shape of the device [12]. Zhang et al. [13] proposed the magnetic design of an MR damper using finite elements. Hitchcock [1] used an FEM software package for magnetic fields and he found that the magnetic field direction should be perpendicular to the MR fluid flow direction. Rosenfeld and Wereley [5] proposed an optimization method for a volume-constrained MR valve. Their method was an analytical optimization design method for MR valves that relied on the assumption of constant magnetic flux density through the magnetic circuit. Nguyen et al. [9] improved an optimization procedure to find the optimal geometric dimensions of the flow ducts and coils to minimize the valve ratio, which is an objective function, for single-coil, two-coil, three-coil, and radial/annular types of MR valves. Nguyen et al. [8] proposed a similar model for MR valves but considered the control energy as well as the time response. Yang et al. [7] offered an optimization procedure for MR smart structure design. In their optimization procedure, target force was the objective and the volume fraction, target time constant, magnetic field intensity, wire-winding turns and power loss were chosen as constraints. Nguyen and Choi [14] presented an optimal design method of an MR shock absorber based on finite element analysis to obtain optimal values of the coil width, the flange thickness, the piston radius and the gap width. Karakoc et al. [15] worked on design considerations for building an automotive MR brake. They used FEM to analyze the resulting magnetic circuit and heat distribution within the MR brake and a multidisciplinary design optimization (MDO) procedure to obtain optimal design parameters for maximum braking torque. Grunwald and Olabi [16] presented parametric analyses, using optimization, with magnetic simulations of an MR valve and an MR orifice. Based on these analyses, they designed, fabricated and tested the devices. Tonoli et al. [17] described a design methodology adopted to develop electromagnetic dampers for installation in aero-engines. Case et al. [18] examined several established and novel damper configurations and modified them to improve performance, while minimizing the power draw of the electromagnet using COMSOL multiphysics finite element software. Gupta and Hirani [19] optimized a multidisk MR brake system using torque and weight as the objective functions and geometric dimensions of a conventional hydraulic brake as constraints. In our brief study [20], an MR shock damper was optimized geometrically using the Taguchi experimental design approach. Four parameters were specified for the geometrical optimization of the MR damper. The desired maximum dynamic range was the target value. The analysis was performed using analytical equations instead of experimental data, in contrast to the current study.

This paper is titled 'optimal damper configurations' instead of 'optimal damper geometries' because two parameters, current and

[1]Corresponding author.

Contributed by the Design Automation Committee of ASME for publication in the Journal of Mechanical Design. Manuscript received November 10, 2011; final manuscript received May 17, 2013; published online June 25, 2013. Assoc. Editor: Diann Brei.

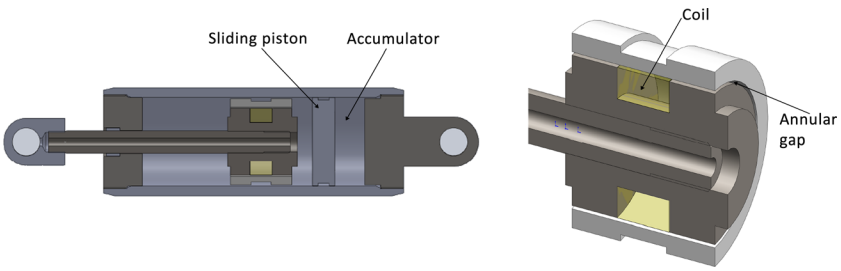

Fig. 1 Schematic for the prototyped MR damper

coil wire diameter, are not part of the geometry; they are related to damper performance. Thus, it is referred to as an optimal configuration that is used to determine the effect of important parameters on damper performance. The optimal configuration of the MR damper is determined using the Taguchi experimental design method, commonly known as the Taguchi method. The Taguchi method creates special arrays to reduce the number of required experiments. Each of the arrays is used for a number of experimental situations and helps experimenters ensure a design that is robust regarding the influence of uncontrollable factors. Four parameters, each of which can be taken at three different levels, were specified for optimal configuration in this study. Eighty-one experiments would have been required for full factorial experiments; nine experiments are adequate using the Taguchi method. Based on the Taguchi method design, nine dampers were fabricated and tested. Optimal damper configurations are specified after reviewing the test results. The target values in the analysis are the maximum dynamic range and the damper force. The gap width, the flange (active pole) length, the coil wire diameter and the current excitation are chosen as the design variables (factors or parameters). The piston gap length, the piston diameter and the piston head housing thickness are constant values. The coil width and height are calculated according to the values of other parameters. The electromagnetic finite element analysis of the magnetic field is used to obtain the magnetic flux density to calculate the yield stress.

2 Design Considerations for the MR Damper

Figure 1 shows a schematic for the prototype MR fluid damper under consideration. Two chambers in the cylinder are separated by a sliding piston. The section where the piston head is filled with MR fluid and the accumulator that compensates for the volume changes induced by the movement of the piston rod is filled with pressurized nitrogen gas. During the motion of the MR damper's piston rod, fluid flows to the other side of the piston head through the annular gap. The coil is located inside the piston head. The coil wire used for winding is heat-resistant and electrically insulated. When electrical current is applied to the coil, a magnetic field occurs around the piston head.

The magnetically induced iron particles inside the MR fluid align in the direction of the magnetic flux lines to resist the flow, thus producing a damping force. In this case, the MR fluid behaves like a non-Newtonian fluid, and the fluid begins to flow after the stress increases higher than the yield stress.

Some of the important dimensions of the magnetic circuit of the MR damper with one coil and annular gap are shown in Fig. 2. The damper geometry is characterized by the gap length, L, the piston head housing thickness, g_h, the annular gap width, g, the flange (active pole) length, t, the piston head radius, R, the radius of the piston core, R_c and the coil width, W. At the two ends of the flanges, the flux lines are perpendicular to the flow direction, causing a field-dependent resistance to the flow.

The total force generated by an MR damper consists of three components: the viscous force (uncontrollable force) from the viscous effects, F_μ, the frictional force, F_f and the field-dependent force (controllable force), F_τ, from the magnetic field [12]

$$F = F_\mu + F_\tau + F_f \tag{1}$$

where

$$F_\mu = Q\frac{6\mu L A_p}{\pi R_1 g^3} \tag{2}$$

and

$$F_\tau = 2c\frac{t}{g}A_p\tau_y \mathrm{sgn}(u_p) \tag{3}$$

where u_p is the piston velocity, A_p is the cross-sectional area of the piston head, Q is the flow rate, μ is the plastic viscosity, $R_1 = R - (g_h + 0.5g)$ is the average radius of the annular gap, τ_y is the yield stress and c is the coefficient that depends on the flow velocity profile with a value ranging from 2.07 to 3.07. Spencer et al. [3] proposed the following approximate relation for the coefficient c

$$c = 2.07 + \frac{6Q\mu}{6Q\mu + 0.4\pi R_1 g^2 \tau_y} \tag{4}$$

and the dynamic range, D, is defined as the ratio of the total damper force to the uncontrollable force as follows:

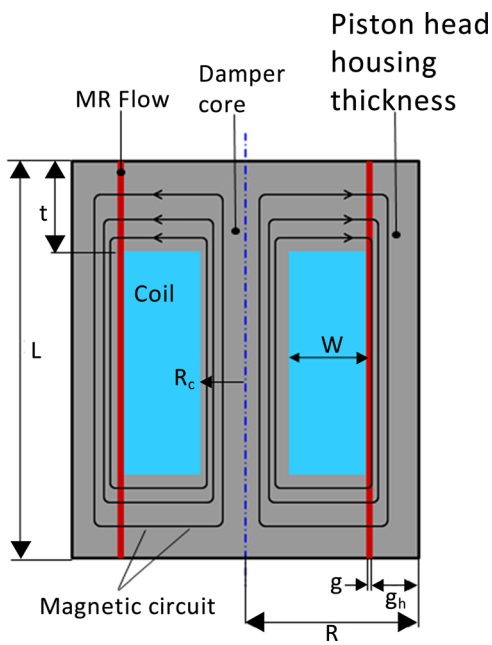

Fig. 2 Magnetic circuit of the MR damper

$$D = 1 + \frac{F_\tau}{F_\mu + F_f} \tag{5}$$

The dynamic range is introduced to evaluate the overall performance of an MR damper, i.e., it is desired to keep D as large as possible to maximize the effectiveness of an MR damper.

As shown in Eqs. (2) and (3), the viscous force increases two orders of magnitude faster than the controllable force with a small gap size if one assumes that the magnetic field is saturated; consequently, the dynamic range tends to zero. As the gap size increases, both the controllable force and the viscous force decrease. To obtain a sufficient amount of controllable force, the gap has to be quite narrow. Note that the friction force is a constant; therefore, the dynamic range tends to zero. Between the extremes, an optimal dynamic range exists. The viscous force is independent of the influence of the magnetic field. The controllable force, however, depends on the yield stress (equation 3). The variation of the active pole length (t) influences the MR fluid via the magnetic field. The pole length has an influence directly on the controllable force but also indirectly on the uncontrollable force via the piston length, L [12].

Parameters such as the piston radius, the yield stress, the pole length and the gap width play important roles in searching for the optimal design.

An important stage in the design considerations of an MR damper is the calculation of the changes in the yield stress of the MR fluid from the magnetic field. In this study, the hydrocarbon-based MR fluid product (MRF-132DG) from the Lord Corporation, Cary, NC, USA is used. Applying the least-squares curve fitting method to the fluid property specifications [21], the yield stress equation is as follows:

$$\tau_y = 52.962B^4 - 176.51B^3 + 158.79B^2 + 13.708B + 0.1442 \tag{6}$$

In equation (6), the unit of the yield stress, τ_y, is kPa and the unit of magnetic flux density, B, are Tesla (T).

The various critical areas though which the magnetic field passes can be of the same size. The assumption of constant magnetic flux density throughout the magnetic circuit of the damper is as follows [5]:

$$\begin{aligned} W &= -(g + R_c) + \sqrt{R^2 - R_c^2} \\ t &= \frac{1}{2}R_c \\ g_h &= R - (W + g + R_c) \end{aligned} \tag{7}$$

3 Determination of MR Dampers for Experimental Design

Design of experiments (DOE) is a statistical technique used to study the effects of multiple variables simultaneously. For planning experiments using the Taguchi experimental design approach, special orthogonal arrays are developed to make the DOE technique more applicable by reducing the number of experiments [22]. In addition, using the signal-to-noise ratio in the analysis of repeated results helps experimenters easily assure a design that is robust to the influence of uncontrollable factors [22]. Taguchi strongly recommends use of signal-to-noise ratio (S/N) to capture the variability of data within the group, thus measuring a quality characteristic prior to determining optimum conditions. Taguchi proposed three S/N equations; depending on the desirability of the results, the quality characteristic can be of type bigger is better, smaller is better, or nominal is best (see Table 1).

Assume that y_i is the ith test value and y_0 is the target test value. When the S/N is increased, variation around the target value decreases; thus, a higher S/N is desirable. Regardless of the original results, the desirability of S/N is always retained as bigger is better.

Table 1 Signal-to-noise (S/N) ratio equations

Quality characteristic	S/N ratio
Smaller is better	$-10\log\left(\frac{1}{n}\sum y_i^2\right)$
Nominal is best	$-10\log\left(\frac{1}{n}\sum (y_i - y_0)^2\right)$
Bigger is better	$-10\log\left(\frac{1}{n}\sum \frac{1}{y_i^2}\right)$

Table 2 Parameters and levels

Parameters	Level 1	Level 2	Level 3
Gap width (g)	0.6 mm	0.8 mm	1 mm
Flange length (t)	5 mm	6 mm	7 mm
Coil wire diameter (d_c)	0.45 mm	0.4 mm	0.35 mm
Current (I)	1 A	1.25 A	1.5 A

A noticeable dynamic range as described by equation (4) is a key objective for MR damper performance because of a large ratio of controllable force to uncontrollable force. The main objective of an MR damper is to increase the controllable force in proportion to the uncontrollable force. The other objective is to increase the damper force, with as much controllability as possible. These reasons drive the dynamic range and damper force to be maximized as two primary objectives of the study.

The gap width, the flange length, the coil wire diameter and the current excitation are design parameters, with three different values, and are used to obtain optimum damper performance (see Table 2). The gap length, the piston rod diameter, the piston core diameter, the inner diameter of the cylinder, the sliding piston width and the inner length of the cylinder are constants, for manufacturing simplicity. The coil width is calculated using equation (7). The number of turns of the coil is calculated using the coil width. The magnetic flux density is obtained through FEM analysis using the parameters specified and calculated.

The parameters and their levels were determined by the Taguchi method realized with some analytical calculations, yield stress from equation (6), the total damper force from equation (1), the dynamic range from equation (5) and the coil width and flange length from equation (7). It is important to specify the parameters to minimize the fabrication difficulty of the dampers. A large number of parameters, which must be specified to achieve the optimal geometry in the manufacture of a large number of dampers, would lead to a much higher cost.

An L9 orthogonal array is suitable for four parameters and three levels, and nine damper models are fabricated and analyzed in accordance with Taguchi's L9 array (see Table 3).

The coil width and the number of turns that is implemented to form a maximum wrap in the coil housing that has 0.5 mm and 1 mm insulation material on the inner and outer faces, respectively, is shown in Table 4.

3.1 Magnetic Flux Density and Yield Stress of the MR Dampers. As shown in Fig. 2, the MR damper is shaped to guide the magnetic flux axially through the bobbin, across the bobbin flange (active pole) length and gap at one end, through the flux return, and across the gap and bobbin flange again at the opposite

Table 3 Factors assigned to L9 orthogonal array

Damp. No.	g (mm)	t (mm)	d_c (mm)	I (A)
1	0.6	5	0.45	1
2	0.6	6	0.4	1.25
3	0.6	7	0.35	1.5
4	0.8	5	0.4	1.5
5	0.8	6	0.35	1
6	0.8	7	0.45	1.25
7	1	5	0.35	1.25
8	1	6	0.45	1.5
9	1	7	0.4	1

Table 4 Coil width and number of turns

Damp. No	W (mm)	N_c
1	4.9	220
2	4.9	233
3	4.9	241
4	4.7	266
5	4.7	292
6	4.7	138
7	4.5	325
8	4.5	164
9	4.5	166

end. The fluid volume though which the magnetic field passes is defined as the active volume. MR effects only occur within this active volume. An effective damper must have a high magnetic flux density passing through a large active volume. However, large numbers of magnetic coils are required to produce large magnetic fields. An optimized circuit would maintain a balance between the field produced and power required by the magnetic coils [5].

The magnetic flux density in the dampers was calculated by FEM analysis, implementing the magnetostatic tool in ANSYS v12.1. For computational time reduction and assuming the magnetic flux to be axisymmetric, the 3D model is a 45 deg slice of the entire computational domain. To model the geometry, some of the dimensions were defined as parameters in ANSYS to easily manipulate all of the required damper geometries in the experimental design. To accommodate the various damper dimensions, a computational domain of approximately 90.000 nodes and 64.000 tetrahedral volume elements is implemented to solve the magnetic analysis problem (see Fig. 3).

After obtaining magnetic flux density (B) at the same point in the gap for all the dampers by ANSYS analysis, the yield stresses (τ_y) are calculated from equation (6) (see Table 5).

Dampers with high magnetic flux density in the gap (see Table 5) are already high in their core region, as shown in Fig. 4. Some analyses performed with ANSYS show the changes in magnetic flux density with the parameters specified in the experimental design (see Fig. 5).

4 Fabrication of the MR Dampers

The candidate MR dampers are fabricated using the dimensions in Table 3, as specified by the Taguchi method. The other dimensions, shown in Table 6, are fixed for all dampers.

The MR damper consists of seven-parts, a cylinder, a piston rod, coil housing, a piston head, an upper and bottom cover for the cylinder and a sliding piston. Approximately 50 mm^3 of MR fluid is filled without any air space in the cylinder volume, and approximately 20 bar of nitrogen is injected into the accumulator. The dampers, after assemblage, are shown in Fig. 6.

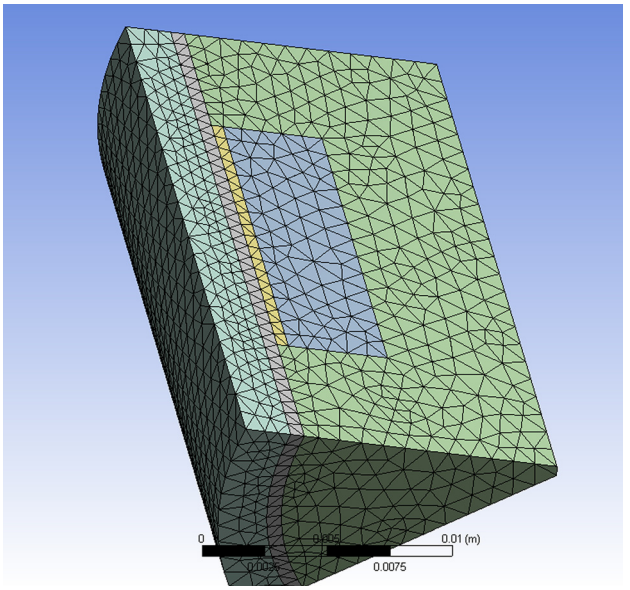

Fig. 3 Mesh of the piston head

Table 5 Values of magnetic flux density and yield stress in the annular gap

Damp. No.	B (T)	τ_y (Pa)
1	0.563	32.02
2	0.505	28.34
3	0.454	24.83
4	0.561	31.93
5	0.454	24.89
6	0.411	21.89
7	0.503	28.16
8	0.463	25.45
9	0.365	18.70

5 Test Set-Up

The prototype dampers are tested on a mechanical scotch yoke-type shock machine Roehrig MK-2150. The shock machine has built-in software (SHOCK 6.3) to collect data from the data card. The output data curves are force versus time, force versus velocity and force versus displacement. The machine has also an IR temperature sensor to read the temperature data during the tests. The primary components of the experimental set-up are shown in Fig. 7. A programmable GWinstek PPE 3223 power supply is used to provide current to the coil of the MR damper.

The dampers are fixed to the machine using grippers, as shown in Fig. 7. The dynamic tests of the dampers are performed under current excitation, while maintaining the velocity and stroke at constant levels of 0.05 m/s and 15 mm, respectively. Force versus time, force versus displacement and force versus velocity curves are obtained and the temperature, the gas force and the friction force are measured for each test. The tests are repeated three times.

6 Optimal Damper Configurations

The dynamic range and damper force are specified as response values in the Taguchi method. It is desired that the values be as large as possible for best damper performance. Therefore, "Bigger is Best" is specified as the S/N equation. Rebound and compression damper forces are measured at the piston position in the middle of the stroke, i.e., piston maximum velocity. The dynamic range is calculated using the damper force with zero applied

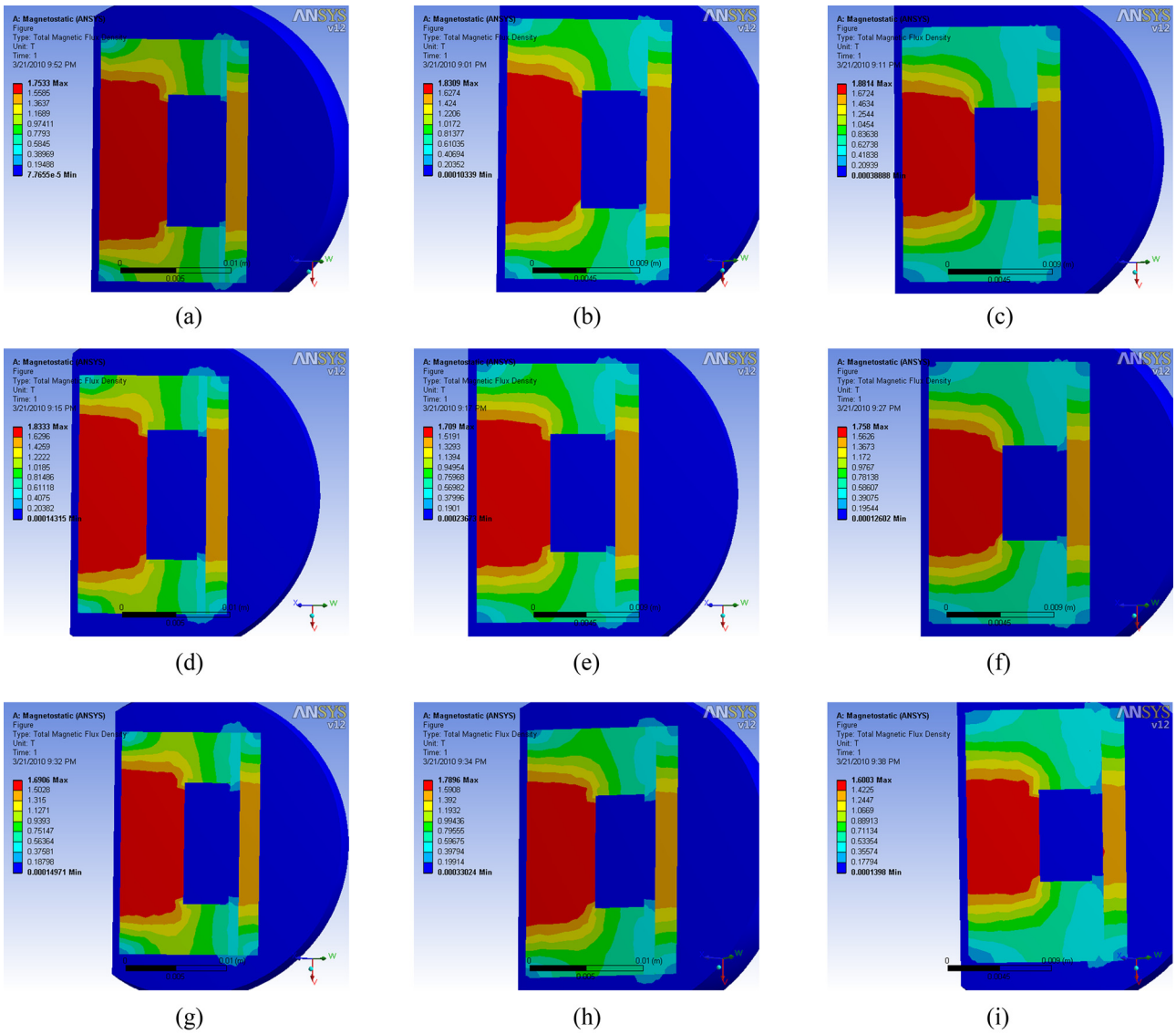

Fig. 4 Magnetic flux densities for (*a*) damper 1, (*b*) damper 2, (*c*) damper 3, (*d*) damper 4, (*e*) damper 5, (*f*) damper 6, (*g*) damper 7, (*h*) damper 8, and (*i*) damper 9

magnetic field. Two Taguchi analyses are applied to two targets, maximum dynamic ratio and maximum damper force. Tests are repeated for three different sets of values to assure a design that is insensitive to the influence of uncontrollable factors.

6.1 Optimum Configuration for Maximum Damper Force. The damper forces for each test, reported as the average of the absolute values of compression and rebound, and the signal/noise (S/N) for each damper are shown in Table 7. S/N for each level of the parameters is listed in Table 8.

As explained above, higher S/N is desirable, specified the best levels of the parameters are shown in Table 9.

Interaction among factors is quite common. A good understanding of the interaction between two factors is highly effective in interpreting experimental results. Therefore, it is important to design experiments to include interactions and to analyze results to determine if interactions are present, whether they are significant, and which factor levels are most desirable [22]. Interactions among factors for this study are shown in Table 10.

The goal of the experimental design is to find ways to control and to reduce the variance of the product. To this end, the parameters that affect performance are determined. The effect of each individual parameter on the results is determined by using a variance of analysis (ANOVA). The ANOVA is a statistical tool and a mathematical technique that separates the components of the total variation. The primary objective of an ANOVA is to extract from the results the degree of variation caused by each factor relative to the total variation in evidence [22]. Results of the ANOVA analysis are shown in Table 11, highlighting the effect of each factor on the performance of the MR damper.

The degree of freedom (DOF) is an indication of the amount of information contained in a data set. The sum of square (S) is the total variation calculated by adding deviations of the individual data points from the mean value. The variance (V) is the sum of the squares per DOF [22].

According to the results of the ANOVA analysis, to reach maximum damper force, the most significant parameter is the gap width, contributing 81.39% followed by the flange, at 8.053%. The coil wire diameter is the least significant parameter, contributing 2.926%. The individual factor influences are properly referred to as the relative percentage influences.

The confidence interval (C.I.) represents the boundaries on the expected results. In this case, C.I. specifies the boundaries of the expected performance at the optimum condition.

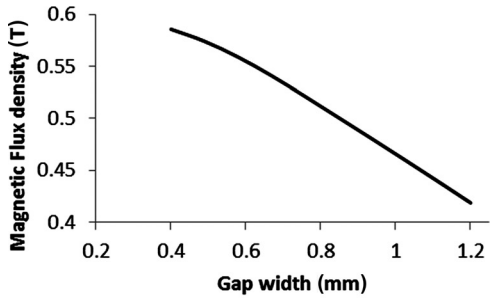

(a)

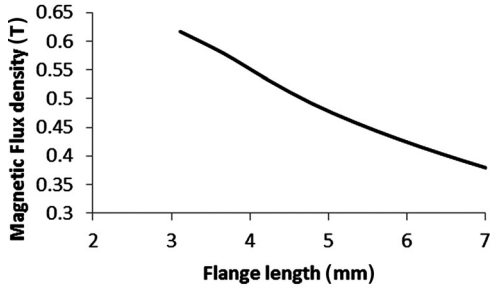

(b)

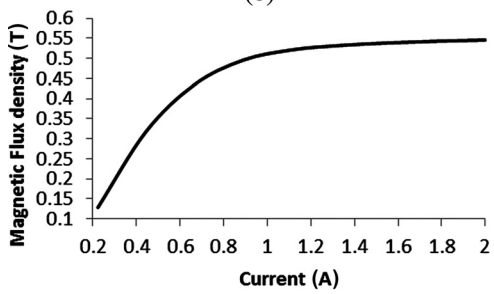

(c)

Fig. 5 (*a*) Curve, magnetic flux density versus gap width, (*b*) curve, magnetic flux density versus flange length, and (*c*) curve, magnetic flux density versus current

Table 6 MR damper constant dimensions

Gap length	22 mm
Piston rod diameter	8 mm
Piston core diameter	14 mm
Inner diameter of cylinder	32 mm
Sliding piston width	8 mm
Inner length of cylinder	80 mm

C.I. formula is as follows:

$$\text{C.I.} = \pm\left[\frac{F(1,n_2)\times V_e}{N_e}\right]^{0.5} = \pm 1.42 \text{ for confidence level } 90\% \tag{8}$$

where $F(1,n_2)$ is the F value from the F table, V_e is the variance of the error term (from ANOVA) and N_e is the effective number of replications. A 90% confidence level indicates that 9 out of 10 times, the averages of the sets are expected to fall within these limits.

According to the values in Table 8, the predicted S/N for the overall optimum condition is as follows:

$$\begin{aligned} \text{S/N}_{\text{predicted}} &= \text{S/N}_{g,1} + \text{S/N}_{t,1} + \text{S/N}_{dc,3} + \text{S/N}_{c,3} - 3\bar{T} \\ \text{S/N}_{\text{predicted}} &= 57.558 + 55.549 + 55.455 + 55.629 - 3\frac{494.68}{9} \\ &= 59.30 \end{aligned} \tag{9}$$

Fig. 6 Dampers after assembling

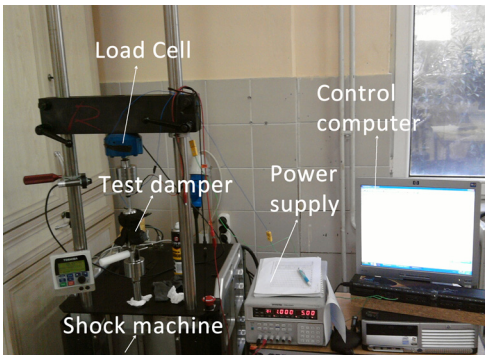

Fig. 7 The test machine with the damper under test

Table 7 Average damper forces and S/N ratios

Damp. No.	Test 1	Test 2	Test 3	S/N
1	873.06	809.65	816.02	58.397
2	732.61	662.37	625.91	56.514
3	854.12	760.07	721.56	57.762
4	660.86	612.73	583.16	55.798
5	698.93	636.10	601.77	56.150
6	463.78	451.89	459.95	53.226
7	427.05	421.96	409.63	52.452
8	482.80	459.76	450.77	53.328
9	378.70	352.08	342.76	51.051

Table 8 S/N ratios of the each level of the parameters

Level	g	t	d_c	I
1	57.55	55.54	54.98	55.19
2	55.05	55.33	54.45	54.06
3	52.27	54.01	55.45	55.62

Table 9 Specified optimum levels of the parameters

Parameter	Optimum level	Optimal value
g	1	0.6 mm
t	1	5 mm
d_c	3	0.35 mm
I	3	1.5 A

Table 10 Interactions among parameters

Interacting factor pairs	Severity index (%)
C. wire diameter × current	72.37
Flange length × current	42.94
Flange length × C. wire diameter	39.37
Gap width × C. wire diameter	30.32
Gap width × flange length	15.21
Gap width × current	7.08

Table 11 ANOVA computation

	DOF	S	V	P %
g	2	41.87	20.93	81.39
t	2	4.14	2.07	8.053
d_c	2	1.50	0.75	2.926
I	2	3.92	1.96	7.631

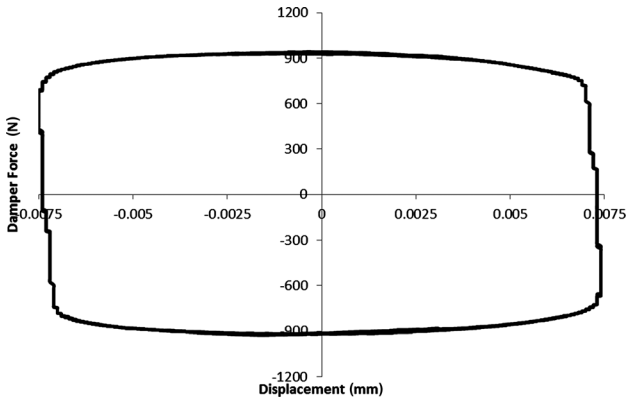

Fig. 8 Force–displacement curve of the optimal damper

Therefore, for a 90% confidence level, the CI is $(59.30 - 1.42) < \mathrm{S/N} < (59.30 + 1.42)$

The expected interval for the optimal condition for the damper force is $783.51N < F < 1086.55N$.

A verification test is conducted to verify that the optimal condition actually produces the desired responses.

6.1.1 Verification Test for Maximum Damper Force Analysis. The damper for the optimal configuration obtained from the Taguchi method performed for the maximum damper force is fabricated and tested. The force–displacement curve for the optimal damper is shown in Fig. 8.

The interval of damper force for the optimal configuration is predicted to be $783.51\ N < F < 1086.55\ N$. As shown in Fig. 8, the damper force, as the average of the absolute values of compression force and rebound force, at the middle of the stroke, i.e., at piston maximum velocity, is approximately $F = 947\ N$. This shows that the Taguchi analysis is verified. The dynamic range of the damper is calculated as $D = 6.79$.

6.2 Optimum Configuration for Maximum Dynamic Range. S/N, calculated according to the values of dynamic range is shown in Table 12. S/N for each level of the parameters is calculated and listed in Table 13.

Optimal levels of the parameters, interaction among the factors and results of the ANOVA analysis are shown in Tables 14–16, respectively.

The ANOVA analysis results show that to reach the maximum dynamic range the most significant parameter is the current excitation, contributing 55.469%, followed by the gap width, at 35.734%. The flange length is the least significant parameter, contributing 0.315%.

Table 12 Dynamic ranges and S/N ratios

Damp. No.	Test 1	Test 2	Test 3	S/N
1	6.26	6.25	5.39	15.45
2	4.37	4.16	3.96	12.36
3	5.91	5.72	5.88	15.31
4	6.91	6.21	6.00	16.04
5	8.87	7.09	6.31	17.15
6	5.63	5.48	4.97	14.54
7	4.77	4.73	4.23	13.16
8	6.25	5.21	4.93	14.61
9	6.32	4.99	4.72	14.35

Table 13 S/N ratios of the each level of the parameters

Level	g	t	d_c	I
1	14.38	14.88	14.87	15.65
2	15.91	14.71	14.25	13.36
3	14.04	14.74	15.21	15.32

Table 14 Specified optimum levels of the parameters

Parameter	Optimum level	Optimal value
g	2	0.8 mm
t	1	5 mm
d_c	3	0.35 mm
I	1	1 A

Table 15 Interactions among parameters

Interacting factor pairs	Severity index (%)
Gap width × C. wire diameter	47.87
Gap width × flange length	43.83
Flange length × C. wire diameter	29.63
Flange length × current	26.11
C. wire diameter × current	11.25
Gap width × current	4.92

Table 16 ANOVA computation

	DOF	S	V	P %
G	2	5.95	2.97	35.73
t	2	0.05	0.02	0.31
d_c	2	1.41	0.70	8.48
I	2	9.24	4.62	55.46

C.I. is ±0.26 for confidence level 90%. As shown in Table 12, the predicted S/N for the overall optimum condition is as follows:

$$\mathrm{S/N}_{\mathrm{predicted}} = 15.915 + 14.887 + 15.214 + 15.655 - 3\frac{133.02}{9} = 17.33$$

The result is converted to dynamic range as $D = 7.2$. At a 90% confidence level, C.I. is $17.07 < \mathrm{S/N} < 17.59$.

The expected interval for the optimal condition of the dynamic range is $7.13 < D < 7.57$.

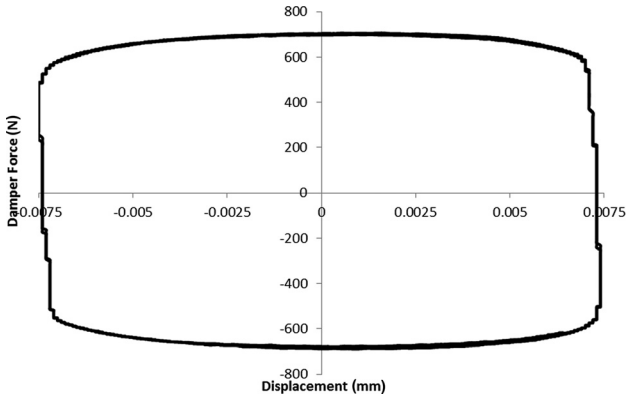

Fig. 9 Force–displacement curve of the optimal damper

6.2.1 Verification Test for Maximum Dynamic Ratio Analysis. The optimally configured damper is fabricated and tested. The force–displacement curve resulting from the test is shown in Fig. 9.

The interval of the dynamic ratio for the optimal configuration was predicted to be $7.13 < D < 7.57$. The actual dynamic range was calculated at approximately $D = 7.37$; thus, the Taguchi analysis is verified. As shown in Fig. 9, the maximum damper force of the optimal damper is approximately $F = 699\ N$.

7 Conclusions

In this study, an experimental design is performed using the Taguchi method with specified parameters, i.e., the gap width, the flange (active) length, the coil wire diameter and the current excitation.

The parameters and their levels were specified according to the Taguchi method analysis. Analytical calculations are performed for the yield stress, the total damper forces, the dynamic range, the coil width and the flange length. The magnetic flux density is calculated from a magnetic saturation FEM analysis. Minimizing the difficulty of the damper fabrication is the most important point in the selection of the parameters.

In the experimental design, nine damper configurations are fabricated and tested. The Taguchi method is implemented to obtain the optimal damper configurations for maximum damper force and dynamic ratio, separately.

The optimal damper configuration obtained in the analysis of the maximum damper force is not one of the actual nine dampers fabricated and tested; it is one of the potential eighty-one combinations. The optimal levels that were specified are: the gap width is 0.6 mm, the flange length is 5 mm, the coil wire diameter is 0.35 mm and the current excitation is 1.5 A. In the ANOVA analysis, for the maximum damper force case, the gap width is the most significant parameter, contributing 81.39% and the coil wire diameter is the least significant parameter, contributing 2.926%. At a confidence level of 90%, the damper force is expected to be in the interval 783.51 N to 1086.55 N. The optimal damper configuration was verified with a damper force of 947 N. The dynamic ratio of the optimal damper is calculated at 6.79 to provide the desired controllability.

The Taguchi method was also used to target the maximum dynamic range. The optimal damper configuration obtained in this analysis is one of the nine dampers already fabricated. The ANOVA analysis of the dynamic range-case shows that the current excitation is the most significant parameter, contributing 55.469% and the flange length is the least significant parameter, contributing 0.315%. The optimal damper configuration was verified with a dynamic range of 7.37, providing the desired controllability also. However, the damper force of the optimal damper was measured as 699 N, which is far from the targeted value. The optimal damper was not verified in terms of target damper force despite the good dynamic range.

In this study, a larger number of parameters could not be analyzed by the Taguchi method, both because of the difficulty and because of the cost of fabricating the dampers. For example, if the piston core diameter and the piston head housing thickness were specified as parameters, the impact of the magnetic circuit on performance could be further investigated. In addition, if the diameter and the length of the piston head could be fabricated using different values, the impact of varying the magnetic field, as a function of the piston head dimensions on performance, could be analyzed. The Taguchi method could be applied to varying velocity and strokes using the same parameters; thus, the impact of velocity and stroke on performance could be examined, separately. In addition, dampers with fixed winding numbers, changing the other geometrical sizes, would provide an experimental design that is insensitive to the magnetic field, taking into account only geometrical quantities.

In this experimental study, it was observed that if the temperature of the damper increases during the test, it has a negative impact on damper performance. It was thought that the heating effect is the uncontrollable factor in the Taguchi analysis and should be minimized in specified optimal configurations. Especially for dampers that use a thinner coil wire, when current excitation increases, temperature increases rapidly. The high temperature causes a variance of viscosity in the MR fluid, affecting damper performance negatively.

Acknowledgment

The authors gratefully acknowledge TUBITAK for making this project possible under Grant Nos. 104M157 and 108M635.

References

[1] Hitchcock, G. H., 2002, "A Novel Magneto–Rhelogical Fluid Damper," Master thesis, Mechanical Engineering Department, Mechanical Engineering University of Nevada, Reno, NV.
[2] Wereley, N. M., and Pang, L., 1998, "Nondimensional Analysis of Semi–Active Electrorheological and Magnetorheological Dampers Using Approximate Parallel Plate Models," Smart Mater. Struct., **7**(5), pp. 732–743.
[3] Spencer, B. F., Jr., Yang, G., Carlson, J. D., and Sain, M. K., 1998, "Smart Dampers for Seismic Protection of Structures: A Full-Scale Study," Second World Conference on Structural Control, Kyoto, pp. 417–426.
[4] Jolly, M. R., Bender, J. W., And Carlson, J. D., 1999, "Properties and Applications of Commercial Magnetorheological Fluids," J. Intell. Mater. Syst. Struct., **10**(1), pp. 5–13.
[5] Rosenfeld, N. C., and Wereley, N. M., 2004, "Volume-Constrained Optimization of Magnetorheological and Electrorheological Valves and Dampers," Smart Mater. Struct., **13**(6), pp. 1303–1313.
[6] Nguyen, Q. H., and Choi, S. B., 2009, "Dynamic Modeling of an Electrorheological Damper Considering the Unsteady Behavior of Electrorheological Fluid Flow," Smart Mater. Struct., **18**(5), p. 055016.
[7] Yang, L., Duan, F., and Eriksson, A., 2008, "Analysis of the Optimal Design Strategy of a Magnetorheological Smart Structure," Smart Mater. Struct., **17**(1), p. 015047.
[8] Nguyen, Q. H., Choi, S. B., and Wereley, N. M., 2008, "Optimal Design of Magnetorheological Valves via a Finite Element Method Considering Control Energy and a Time Constant," Smart Mater. Struct., **17**(2), p. 025024.
[9] Nguyen, Q. H., Han, Y. M., Choi, S. B., and Wereley, N. M., 2007, "Geometry Optimization of MR Valves Constrained in a Specific Volume Using the Finite Element Method," Smart Mater. Struct., **16**(6), p. 2242.
[10] Stanway, R., Sproston, J. L., and El-Wahed, A. K., 1999, "Applications of Electro-Rheological Fluids in Vibration Control: A Survey," Smart Mater. Struct., **5**(4), p. 464.
[11] Namuduri, C. S., Alexandridis, A. A., Madak, J., and Rule, D. S, 2001, "Magnetorheological Fluid Damper With Multiple Annular Flow Gaps," U.S. Patent 6,279,701.
[12] Delivorias, R. P., 2004, "Application of ER and MR Fluid in an Automotive Crash Energy Absorber," MT0418, Eindhoven University of Technology Department of Mechanical Engineering, Eindhoven.
[13] Zhang, H. H., Liao, C. R., Chen, W. M., Huang, S. L., 2006, "A Magnetic Design Method of MR Fluid Dampers and FEM Analysis on Magnetic Saturation," J. Intell. Mater. Syst. Struct., **17**(8–9), pp. 813–818.
[14] Nguyen, Q. H., and Choi, S. B., 2009, "Optimal Design of MR Shock Absorber and Application to Vehicle Suspension," Smart Mater. Struct., **18**(3), p. 035012.

[15] Karakoc, K., Park, E. J., and Suleman, A., 2008, "Design Considerations for an Automotive Magnetorheological Brake," Mechatronics, **18**(8), pp. 434–447.
[16] Grunwald, A., and Olabi, A. G., 2008, "Design of Magneto-Rheological (MR) Valve," Sens. Actuators, A, **148**(1), pp. 211–223.
[17] Tonoli, A., Amati, N., Bonfitto, A., Silvagni, M., Staples, B., and Karpenko, E., 2010, "Design of Electromagnetic Dampers for Aero-Engine Applications," ASME J. Eng. Gas Turbines Power, **132**(11), p. 112501.
[18] Case, D., Taheri, B., and Richer, E., 2011, "Finite Element Modeling and Analysis of Magnetorheological Dampers," ASME 2011 International Mechanical Engineering Congress and Exposition, Vol. 7, Dynamic Systems and Control; Mechatronics and Intelligent Machines, Parts A and B.
[19] Gupta, S., and Hirani, H., 2011, "Optimization of Magnetorheological Brake," ASME/STLE 2011 International Joint Tribology Conference, Los Angeles, California, October 24–26.
[20] Parlak, Z., Engin, T., Arı, V., Şahin, İ., and Çalli, İ., 2010, "Geometrical Optimisation of Vehicle Shock Dampers With Magnetorheological Fluid," Int. J. Veh. Des., **54**(4), pp. 371–392.
[21] Lord Corporation, 2003, "MR Fluid Product Bulletins," from http://www.rheonetic.com/fluidbegin.htm
[22] Roy, R. K., 2003, *Design Experiments Using the Taguchi Aproach:16 Steps to Product and Process. Improvement*, A Wiley–Interscience Publication, New York, NY.